in vivo *35*: 275-281 (2021)
doi:10.21873/invivo.12256

Deformation of the Pelvic Arteries Caused by Pneumoperitoneum and Postural Changes in an Animal Model

HIDEMICHI KIYOMATSU[1], LEI MA[2], JUNCHEN WANG[3], TOMOMICHI KIYOMATSU[1], HIROYUKI TSUKIHARA[2], ETSUKO KOBAYASHI[2], ICHIRO SAKUMA[2] and SOUICHIRO ISHIHARA[1]

[1]*Department of Surgical Oncology, Faculty of Medicine, The University of Tokyo, Tokyo, Japan;*
[2]*Graduate School of Engineering, The University of Tokyo, Tokyo, Japan;*
[3]*School of Mechanical Engineering and Automation, Beihang University, Beijing, P.R. China*

Abstract. *Background/Aim: We investigated pelvic arterial deformation and shift due to intraoperative pneumoperitoneum and postural changes in an animal model. Materials and Methods: Computed tomography images of pigs were acquired in different body positions (supine, head down at 5° and 10°, right lateral recumbent at 5° and 15°) before and after insufflation. We used a free software (3D Slicer) for image analysis. After landmark registration using 10 markers inserted into the pelvis, pelvic arterial deformation and shift of seven arterial bifurcation points were evaluated. The distance moved was the target registration error (TRE) from the points registered in the supine position. Fiducial registration error (FRE) was measured using the 10 pelvic markers. Results: TRE average from postural changes ranged from 0.7 to 1.2 mm and was 1.4 mm due to pneumoperitoneum. TRE and FRE averages were 2.1 mm and 0.2 mm, respectively. Conclusion: The pelvis was useful for registering anatomical landmarks.*

Rectal cancer is associated with a worse prognosis than colon cancer because of its high rate of local recurrence (1). Rectal cancer has a high rate of local recurrence, commonly presenting with lateral pelvic lymph node metastasis. The rates of lateral pelvic lymph node metastasis vary from 10% to 15% (2-4), and they increase with the depth of tumor invasion. A total of 16.5% of patients with T3 tumors and 37.2% of patients with T4 tumors had lateral pelvic lymph node metastasis (5). In Japan, the standard treatment procedure for advanced lower rectal cancer is a total mesorectal excision (TME) and a lateral pelvic lymph node dissection (LPLD) for pelvic lymph node metastasis. The procedure is generally performed with minimally invasive surgery, including laparoscopic and robotic surgery, because of the advantages of decreased postoperative pain, reduced hospitalization, and improved long-term outcome (6). However, the affected lymph nodes are located alongside the pelvic arteries and autonomic nerves; thus, LPLD carries the risk of blood loss and urinary and sexual dysfunction (7). Therefore, we aimed to develop a real-time navigation system to help surgeons perform this procedure more safely and efficiently by comparing the intraoperative images to the preoperative images, such as computed tomography (CT) or magnetic resonance images and displaying the pelvic arteries on the monitor.

Surgical navigation systems were first reported in neurosurgery (8). Surgical navigation systems have become widely prevalent in neurosurgery, as well as in orthopedic, otolaryngologic, and liver surgeries (9-11). For rectal cancer, Atallah *et al.* (12) have assessed transanal TME conducted with navigation, and Nijkamp *et al.* (13) have assessed open pelvic surgery with navigation. However, real-time navigation systems have not yet become widely available for abdominal laparoscopic colorectal surgery. Surgical manipulation such as pneumoperitoneum and postural changes have a considerable effect on the abdominal wall and intra-abdominal organs and introduce movement and deformation, which can affect the accuracy of the navigation systems. However, we thought that deformation of the pelvic arteries due to surgical manipulations would be relatively small, because the pelvic arteries are located against the pelvis.

Nimsky *et al.* (14) have reported an intraoperative brain shift during neurosurgery. Ohya *et al.* (15) reported carotid artery deformation caused by head and neck postural changes during otolaryngologic surgery. Vijayan *et al.* (16) and Zijlmans *et al.*

Correspondence to: Hidemichi Kiyomatsu, Department of Surgical Oncology, Faculty of Medicine, The University of Tokyo, 7-3-1 Hongo, Bunkyo-ku, Tokyo 113-0033, Japan. Tel: +81 338155411 (ext. 33246), Fax: +81 338116822, e-mail: kiyomatsu71@yahoo.co.jp

Key Words: Pelvic artery deformation, navigation, postural changes, pneumoperitoneum.

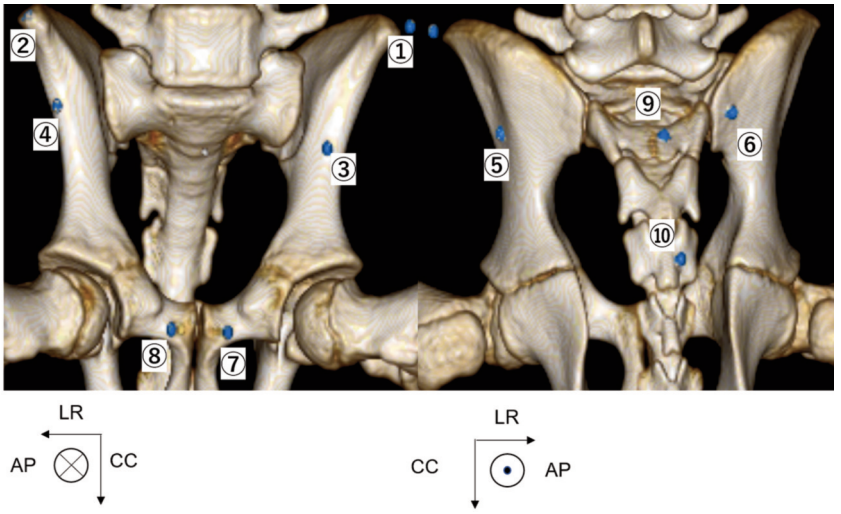

Figure 1. *Three-dimensional computed tomography showing 10 markers (indicated by the 10 numbers) placed around the pelvis. LR: Left-right, AP: anterior-posterior, CC: cranio-caudal.*

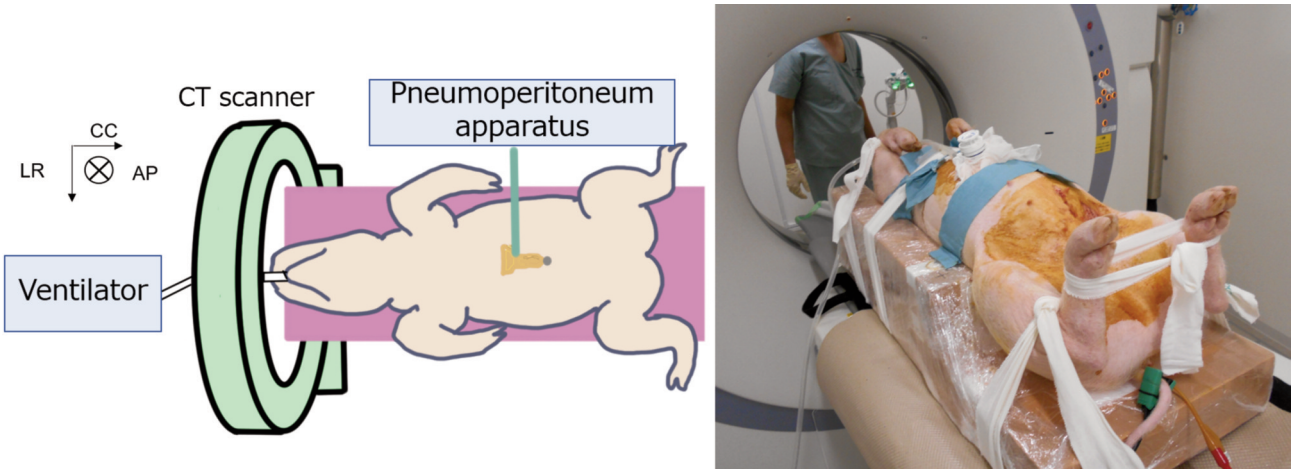

Figure 2. *A schematic and an image of the experimental set-up. LR: Left-right; AP: anterior-posterior; CC: cranio-caudal.*

(17) examined liver deformation due to pneumoperitoneum during liver surgery. These studies used pigs as an animal model. However, to our knowledge, no previous study has examined deformation of the pelvic arteries due to surgical manipulation. The aim of this study was to present a landmark registration method using the pelvis in an animal model, and to provide the first result of deformation of the pelvic arteries caused by pneumoperitoneum and postural changes.

Materials and Methods

Animals and anesthesia. Two pigs (Landrace), with a weight of 36 kg, were used in this study. The pigs were born at the Ibaraki farm (Ibaraki, Japan) approximately 3 months before the study, and housed for 10 days after a 7-day quarantine period. Both pigs were females, because it was easier to place a urethral catheter into the bladder. The urethra of male pigs is long and tortuous, and it is difficult to insert a catheter through it. The pigs fasted one day before the experiment.

The pigs were premedicated with atropine sulfate at a dose of 0.02 mg/kg, midazolam at 0.3 mg/kg, and medetomidine at 0.06 mg/kg 1 h before the start of the experiment. The pigs underwent tracheal intubation after deep anesthesia was induced by sevoflurane. The pigs were then attached to a ventilator with a respiration rate of 12 breaths per min and a tidal volume of approximately 400 ml. All pigs underwent placement of a urethral catheter. Sevoflurane and midazolam were used for the maintenance of general anesthesia. Pulse oximetry, electrocardiography, and non-invasive blood pressure were monitored during the experiment.

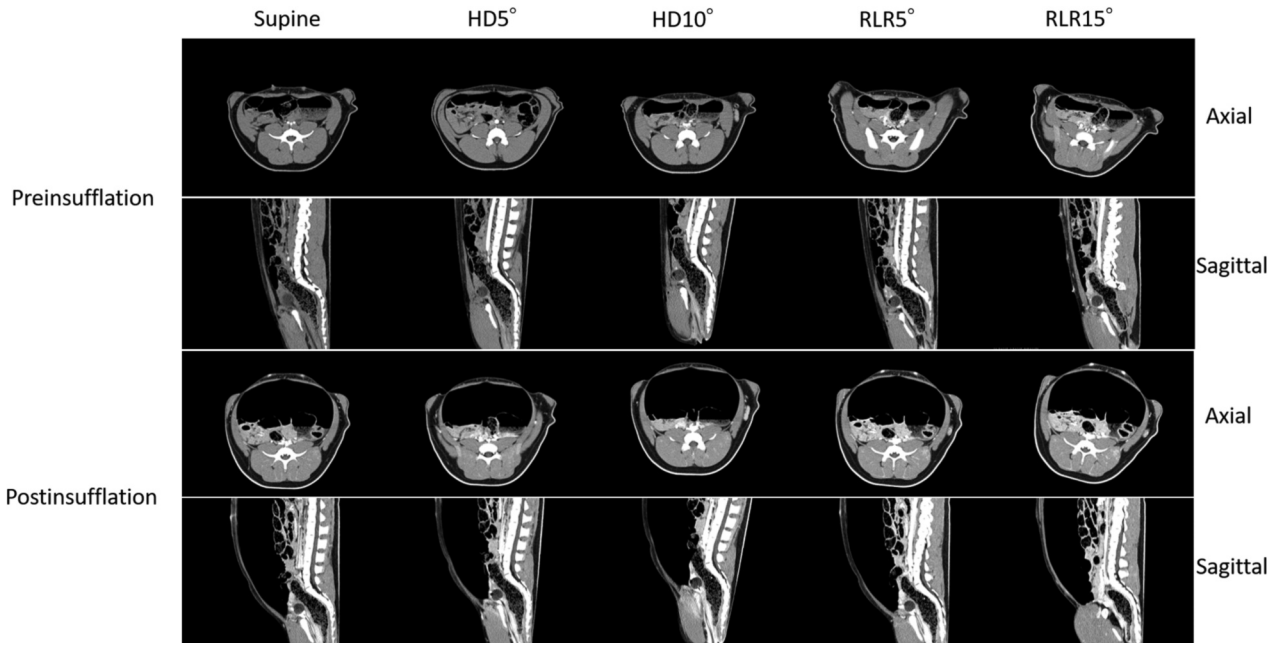

Figure 3. *Upper computed tomography images were acquired under different postural changes (supine, HD 5˚, HD 10˚, RLR 5˚, RLR 15˚). Lower computed tomography images were acquired under pneumoperitoneum and different postural changes. HD: Head down; RLR: right lateral recumbent.*

This study was approved by the President of Tokyo University after a review by the Institutional Animal Care and Use Committee (Permission number: KA15-3) and conducted according to the Tokyo University Animal Experimentation Regulations. This study complied with the ARRIVE guidelines. The study also adhered to the Guiding Principles in the Care and Use of Animals approved by the Council of the American Physiological Society

Surgical procedure and imaging. We made an incision in the abdominal wall above the umbilicus. A trocar was then placed through this site to create the pneumoperitoneum. Ten markers were inserted around the pelvis (both sides of the anterior superior iliac spine, the bilateral anterior and posterior surface of the ilium, both sides of the pubis, and the upper and lower sacrum) using a sliding needle under fluoroscopic guidance, for use as registration markers (Figure 1). The markers were 1-mm steel balls. Figure 2 shows an overview of the experimental set-up. During image acquisition, the pigs were strapped into a Styrofoam platform to keep them stationary.

We used a CT scanner (Somatom Sensation 16®; Siemens Medical Solutions, Erlangen, Germany) to obtain the CT images. On the examining table, the pigs were positioned in the supine position, with their heads facing down (5˚ and 10˚), and to the right lateral recumbent position (RLR) (5˚ and 15˚) by slanting the Styrofoam platform. The slant angle was measured at the same position on the Styrofoam platform using a digital angle gauge. The angle varied within±0.1˚ during image acquisition. After acquiring the CT images according to the postural changes, we created the pneumoperitoneum, and CT images were acquired according to the same postural changes (Figure 3). The target intra-abdominal pressure was set to 10 mmHg. The pressure varied within±1 mmHg during image acquisition. The ventilator flow was terminated at the end of expiration during the CT scanning to acquire the images without the movement caused by respiration. Lohexol, a non-ionic contrast medium, was injected to acquire the arterial phase image. CT image data were acquired as Digital Imaging and Communication in Medicine (DICOM) data. The image resolution was 512×512 pixels, and each pixel was 0.586×0.586 mm^2. The CT slice thickness was 0.7 mm.

Imaging analysis. The 3D Slicer, a free and open source software, was used for visualization and registration of the landmarks (18). Figure 4 shows the workflow of the registration of the landmarks and evaluation that was conducted based on 3D Slicer. First, the CT images, in the DICOM format, were imported into 3D Slicer *via* the `DICOM` module.

Registration. Image registration was used for the alignment of two images of different types (supine, the postural change conditions, and the pneumoperitoneum) from the same animal. Using the 'landmark registration' module in 3D Slicer, 10 markers around the pelvis, which were clearly identified on the CT images, were selected and registered as the landmarks.

Assessment of the deformation of the pelvic arteries. After landmark registration, we calculated the fiducial registration error (FRE) for each marker. Coordinates (X, Y, Z) were obtained for the 10 markers used as landmarks in pre-and post-insufflation and for postural changes. The FRE was determined using the Euclidean distance formula:

$$FRE = \sqrt[2]{(X_{pre} - X_{post})^2 + (Y_{pre} - Y_{post})^2 + (Z_{pre} - Z_{post})^2}$$

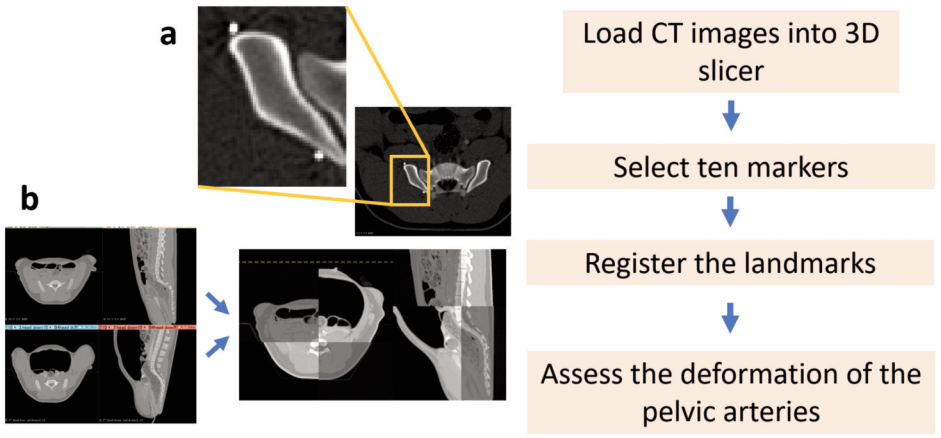

Figure 4. *The workflow of the registration and evaluation system based on 3D Slicer. (a) Select 10 markers and insert them around the pelvis. (b) Register the landmarks of two images of different types (supine, postural change conditions, and pneumoperitoneum).*

FRE is the vector length between the marker positions that are used as the landmarks in pre-and post-insufflation, and in pre-and post-postural change scans; (X_{pre}, Y_{pre}, Z_{pre}) are the CT volume positions of the markers in the supine position before insufflation; and (X_{post}, Y_{post}, Z_{post}) are the CT volume positions of the markers for postural changes or after insufflation. Both volumes are located in the same coordinated system in physical space.

We also assessed the target registration error (TRE) for each of the seven arterial bifurcations. Figure 5 shows seven bifurcations on the three-dimensional blood vessel image that was edited using a CT workstation (Ziostation, Ziosoft Inc., Tokyo, Japan). The coordinates (x, y, z) were obtained for each of the seven arterial bifurcations both before and after insufflation and for the postural changes. The TRE was determined using the Euclidean distance formula:

$$TRE = \sqrt[2]{(x_{pre} - x_{post})^2 + (y_{pre} - y_{post})^2 + (z_{pre} - z_{post})^2}$$

TRE is the vector length between the arterial bifurcation position before and after insufflation and before and after postural change scans; (x_{pre}, y_{pre}, z_{pre}) are the CT volume positions of the arterial bifurcations in the supine position before insufflation; and (x_{post}, y_{post}, z_{post}) are the CT volume positions of the arterial bifurcations for postural changes or after insufflation. Both volumes are located in the same coordinated system in physical space.

Statistical analysis to examine the FRE associated with the 10 landmarks and TRE associated with the seven bifurcations was performed. All data are reported as mean±standard deviation.

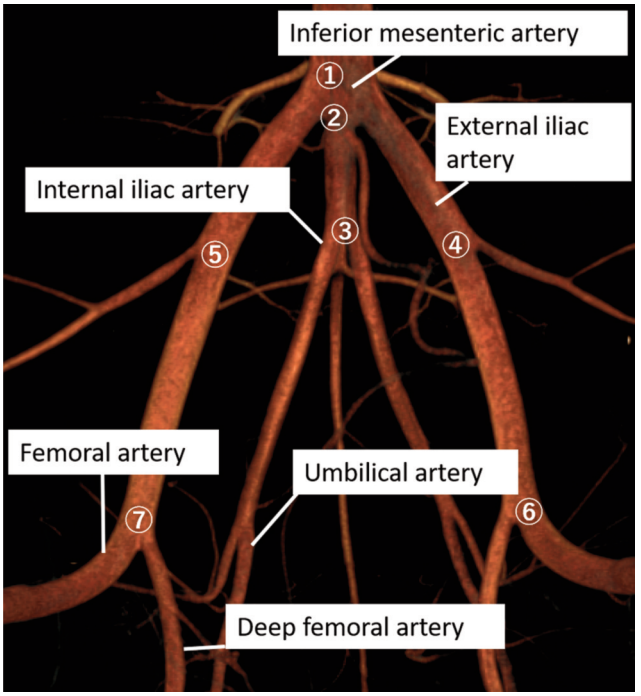

Figure 5. *A three-dimensional blood vessel image that identifies the seven arterial bifurcations in the pelvic arteries (inferior mesenteric, external and internal iliac arteries) is edited using a computed tomography workstation (Ziostation, Ziosoft Inc., Tokyo, Japan).*

Results

The average and standard deviation of the FRE in the supine position, the head down (HD) at 5˚, the HD at 10˚, the RLR at 5˚, and the RLR at 15˚ were examined before and after insufflation. The average FRE was 0.2 mm. The FRE values ranged from 0.1 to 0.3 mm.

Tables I and II show the main findings of this study. Table I includes averages and standard deviations of the TRE in the supine, the HD at 5˚, the HD at 10˚, the RLR at 5˚, and the RLR at 15˚ under pre- and post-insufflation. The TRE values before insufflation ranged from 0.7 to 1.2 mm, and those after insufflation ranged from 1.4 to 2.1 mm. The largest TRE measurement was in the RLR at the 15˚ position under insufflation.

Table I. *Target registration error of seven bifurcations in the supine, head down 5˚ and 10˚, right lateral recumbent position 5˚ and 15˚, under insufflation.*

	Supine	HD5˚	HD10˚	RLR5˚	RLR15˚
Preinsufflation		0.9±0.3	1.0±0.3	0.7±0.3	1.2±0.6
Postinsufflation	1.4±1.0	1.5±9	1.5±0.8	1.7±0.7	2.1±1.0

(n=14).

Table II includes the TRE of each bifurcation in the HD and RLR positions, along with postural changes under insufflation. The range of the TRE of each bifurcation in the HD and RLR under pre-insufflation was approximately 1 mm. However, in postural changes under post-insufflation, the TRE of bifurcations ④ and ⑤ (external iliac arteries) was 2.7 mm and 2.6 mm, respectively.

Table II. *Target registration error of each bifurcation in the head down and right lateral recumbent positions and postural changes under insufflation.*

	HD (n=4)	RLR (n=4)	Postural changes +insufflation (n=8)
Bifurcation①	1.1±0.5	0.9±0.9	1.5±0.7
Bifurcation②	1.0±0.3	1.2±0.4	1.5±0.5
Bifurcation③	0.8±0.2	1.0±0.3	0.9±0.5
Bifurcation④	0.9±0.3	0.9±0.7	2.7±0.8
Bifurcation⑤	1.1±0.3	0.9±0.3	2.6±0.6
Bifurcation⑥	1.0±0.4	0.9±0.1	1.2±0.3
Bifurcation⑦	0.7±0.2	0.9±0.6	1.6±0.5

HD: Head down; RLR: right lateral recumbent.

Discussion

We presented the evaluations of pelvic artery deformations due to pneumoperitoneum and postural changes in an animal model. We used 10 markers inserted around the pelvis for registration. Regarding laparoscopic surgery, the skin and most of the intra-abdominal organs were largely affected by postural change and pneumoperitoneum. Hayashi *et al*. (19) reported a real-time navigation system for laparoscopic gastrectomy using skin-fixed markers. They reported an FRE of 14.0 mm. In addition, it is difficult to locate a permanent attachment of the skin-affixed markers at the same site, yet it is acceptable for patient comfort and cosmetic reasons, because CT is usually performed several weeks before surgery. This study revealed an FRE average of only 0.2 mm, which remained mostly unaffected by pneumoperitoneum and postural changes. Thus, our study suggests that the pelvis provides a useful registration as a landmark. The major problem associated with using the pelvis as a landmark is that it is difficult to insert markers around the pelvis in humans. Pandey *et al*. (20) reported a method that used 3D ultrasound with fast and automatic segmentation and included registration of the pelvis CT, which might be used clinically. Further, the study reported a TRE of 2.4 mm that was achieved with a mean runtime of 27.3 s. This procedure can be rapidly and accurately performed inter-operatively for pelvic registration. In addition, the ultrasound procedure is useful as a less invasive approach for patients.

Therefore, 3D Slicer has been used in various studies in the computer-aided surgery community, and the findings support the development of extension modules. For example, Ungi *et al*. (21) developed a free, open source surgical navigation software module 'SlicerIGT' to improve the success rate and time efficiency of facet joint injections.

For accuracy of the real-time navigation, it is important to demonstrate that the pelvic arteries as targets are slightly displaced by postural changes and pneumoperitoneum. Our results revealed that TRE values ranged from 0.7 to 1.2 mm due to postural changes and that the TRE value was 1.4 mm due to pneumoperitoneum. At maximum, the TRE value was 2.1 mm in the RLR at 15˚ after insufflation. As the angle of postural change increased, the TRE value also increased. However, in most clinical cases, the angles of the HD and RLR positions are no larger than 15˚, because the lung is compressed, and respiratory function is depressed. With respect to each bifurcation, there was no difference in postural changes under pre-insufflation. However, the TRE value for the bilateral bifurcations in the external iliac arteries was 2.7 mm. These findings suggest that the external arteries are slightly affected by pneumoperitoneum. Previous reports found carotid artery deformation and brain shift due to postural change and liver deformation due to pneumoperitoneum (12-15). This study showed that pelvic arterial deformation was significantly reduced compared to the deformations reported in the other studies. We speculate that this is because the pelvic arteries are surrounded by a large bone and remain anchored to the retroperitoneum. Surgeons commented that real-time navigation systems would be useful to perform laparoscopic/robotic surgery if the TREs would be <5 mm. Pelvic arterial deformation due to postural change and pneumoperitoneum meets this

requirement. For this reason, the pelvic arteries are a possible target for real-time navigation systems. As part of a new era of laparoscopic and robotic surgery, the images of the pelvic arteries could be projected onto an intraoperative screen during LPLD for rectal cancer.

However, we used an animal model. Human anatomy differs slightly from the pig in the size and configuration of the pelvis and the course of the pelvic arteries. The pelvis of a human that walks on two legs is more free-ranging and the pelvic floor muscles are thicker than those of a pig that walks on four legs. Therefore, we consider that in humans, the pelvic arterial deformations are smaller than those in pigs. In the future, human clinical studies will be needed.

Conclusion

In this study, we presented a new model to evaluate the deformation of the pelvic arteries due to postural change and pneumoperitoneum, and a method to register landmarks of the pelvis using 3D Slicer. This is the first study to demonstrate that the deformation of the pelvic arteries caused by pneumoperitoneum and postural changes was ≤2.1 mm. The pelvis was useful to register landmarks. In a real-time navigation system for LPLD, this finding contributes considerably to registration between intraoperative and preoperative images. Future work including human clinical studies is warranted to evaluate deformation of the pelvic arteries.

Funding

JSPS KAKENHI Grant Number 26108008, JSPS- NSFC Joint Research Project JPJSBP 120197410, and JST COI Grant Number JPMJCEJPMJCE1304

Conflicts of Interest

The Authors have no conflicts of interest to declare regarding this study.

Authors' Contributions

Concept: Hidemichi Kiyomatsu; Design: Hidemichi Kiyomatsu; Supervision: Etsuko Kobayashi, Ichiro Sakuma, Souichiro Ishihara; Data collection and/or processing: Hidemichi Kiyomatsu, Lei Ma; Analysis and/or interpretation: Hidemichi Kiyomatsu; Literature review: Hidemichi Kiyomatsu, Etsuko Kobayashi, Ichiro Sakuma; Writing: Hidemichi Kiyomatsu; Critical review: Hidemichi Kiyomatsu, Junchen Wang, Tomomichi Kiyomatsu, Hiroyuki Tsukihara.

Acknowledgements

The Authors would like to thank Kazuhiro Endo and Syuuji Hishikawa at the Centre for Development of Advanced Medical Technology, Jichi Medical University, Japan for supporting this animal study.

References

1 Watanabe T, Muro K, Ajioka Y, Hashiguchi Y, Ito Y, Saito Y, Hamaguchi T, Ishida H, Ishiguro M, Ishihara S, Kanemitsu Y, Kawano H, Kinugasa Y, Kokudo N, Murofushi K, Nakajima T, Oka S, Sakai Y, Tsuji A, Uehara K, Ueno H, Yamazaki K, Yoshida M, Yoshino T, Boku N, Fujimori T, Itabashi M, Koinuma N, Morita T, Nishimura G, Sakata Y, Shimada Y, Takahashi K, Tanaka S, Tsuruta O, Yamaguchi T, Yamaguchi N, Tanaka T, Kotake K, Sugihara K and Japanese Society for Cancer of the Colon and Rectum: Japanese Society for Cancer of the Colon and Rectum (JSCCR) guidelines 2016 for the treatment of colon cancer. Int J Clin Oncol *23(1)*: 1-34, 2018. PMID: 28349281. DOI: 10.1007/s10147-017-1101-6

2 Sugihara K, Moriya Y, Akasu T and Fujita S: Pelvic autonomic nerve preservation for patients with rectal carcinoma. Oncologic and functional outcome. Cancer *78(9)*: 1871-1880, 1996. PMID: 8909305.

3 Ueno H, Mochizuki H, Hashiguchi Y and Hase K: Prognostic determinants of patients with lateral nodal involvement by rectal cancer. Ann Surg *234(2)*: 190-197, 2001. PMID: 11505064. DOI: 10.1097/00000658-200108000-00008

4 Ueno M, Oya M, Azekura K, Yamaguchi T and Muto T: Incidence and prognostic significance of lateral lymph node metastasis in patients with advanced low rectal cancer. Br J Surg *92(6)*: 756-763, 2005. PMID: 15838895. DOI: 10.1002/bjs.4975

5 Kobayashi H, Mochizuki H, Kato T, Mori T, Kameoka S, Shirouzu K and Sugihara K: Outcomes of surgery alone for lower rectal cancer with and without pelvic sidewall dissection. Dis Colon Rectum *52(4)*: 567-576, 2009. PMID: 19404054. DOI: 10.1007/DCR.0b013e3181a1d994

6 Darzi SA and Munz Y: The impact of minimally invasive surgical techniques. Annu Rev Med *55*: 223-237, 2004. PMID: 14746519. DOI: 10.1146/annurev.med.55.091902.105248

7 Fujita S, Akasu T, Mizusawa J, Saito N, Kinugasa Y, Kanemitsu Y, Ohue M, Fujii S, Shiozawa M, Yamaguchi T, Moriya Y and Colorectal Cancer Study Group of Japan Clinical Oncology Group: Postoperative morbidity and mortality after mesorectal excision with and without lateral lymph node dissection for clinical stage II or stage III lower rectal cancer (JCOG0212): results from a multicentre, randomised controlled, non-inferiority trial. Lancet Oncol *13(6)*: 616-621, 2012. PMID: 22591948. DOI: 10.1016/S1470-2045(12)70158-4

8 Watanabe E, Watanabe T, Manaka S, Mayanagi Y and Takakura K: Three-dimensional digitizer (Neuronavigator): new equipment for computed tomography-guided stereotaxic surgery. Surg Neurol *27(6)*: 543-547, 1987. PMID: 3554569. DOI: 10.1016/0090-3019(87)90152-2

9 Nakamura N, Nishii T, Kitada M, Iwana D and Sugano N: Application of computed tomography-based navigation for revision total hip arthroplasty. J Arthroplasty *28(10)*: 1806-1810, 2013. PMID: 23523215. DOI: 10.1016/j.arth.2012.11.015

10 Kohan D and Jethanamest D: Image-guided surgical navigation in otology. Laryngoscope *122(10)*: 2291-2299, 2012. PMID: 22961537. DOI: 10.1002/lary.23522

11 Peterhans M, vom Berg A, Dagon B, Inderbitzin D, Baur C, Candinas D and Weber S: A navigation system for open liver surgery: design, workflow and first clinical applications. Int J Med Robot *7(1)*: 7-16, 2011. PMID: 21341357. DOI: 10.1002/rcs.360

12 Atallah S, Parra-Davila E, Melani AGF, Romagnolo LG, Larach SW and Marescaux J: Robotic-assisted stereotactic real-time navigation: initial clinical experience and feasibility for rectal cancer surgery. Tech Coloproctol *23(1)*: 53-63, 2019. PMID: 30656579. DOI: 10.1007/s10151-018-1914-y

13 Nijkamp J, Kuhlmann KFD, Ivashchenko O, Pouw B, Hoetjes N, Lindenberg MA, Aalbers AGJ, Beets GL, van Coevorden F, KoK N and Ruers TJM: Prospective study on image-guided navigation surgery for pelvic malignancies. J Surg Oncol *119(4)*: 510-517, 2019. PMID: 30582622. DOI: 10.1002/jso.25351

14 Nimsky C, Ganslandt O, Cerny S, Hastreiter P, Greiner G and Fahlbusch R: Quantification of, visualization of, and compensation for brain shift using intraoperative magnetic resonance imaging. Neurosurgery *47(5)*: 1070-1079, 2000. PMID: 11063099. DOI: 10.1097/00006123-200011000-00008

15 Ohya T, Iwai T, Luan K, Kato T, Liao H, Kobayashi E, Mitsudo K, Fuwa N, Kohno R, Sakuma I and Tohnai I: Analysis of carotid artery deformation in different head and neck positions for maxillofacial catheter navigation in advanced oral cancer treatment. Biomed Eng Online *11*: 65, 2012. PMID: 22947045. DOI: 10.1186/1475-925X-11-65

16 Vijayan S, Reinertsen I, Hofstad EF, Rethy A, Hernes TA and Langø T: Liver deformation in an animal model due to pneumoperitoneum assessed by a vessel-based deformable registration. Minim Invasive Ther Allied Technol *23(5)*: 279-286, 2014. PMID: 24848136. DOI: 10.3109/13645706.2014.914955

17 Zijlmans M, Langø T, Hofstad EF, Van Swol CF and Rethy A: Navigated laparoscopy-liver shift and deformation due to pneumoperitoneum in an animal model. Minim Invasive Ther Allied Technol *21(3)*: 241-248, 2012. PMID: 22455616. DOI: 10.3109/13645706.2012.665805

18 Fedorov A, Beichel R, Kalpathy-Cramer J, Finet J, Fillion-Robin JC, Pujol S, Bauer C, Jennings D, Fennessy F, Sonka M, Buatti J, Aylward S, Miller JV, Pieper S and Kikinis R: 3D Slicer as an image computing platform for the Quantitative Imaging Network. Magn Reson Imaging *30(9)*: 1323-1341, 2012. PMID: 22770690. DOI: 10.1016/j.mri.2012.05.001

19 Hayashi Y, Misawa K, Oda M, Hawkes DJ and Mori K: Clinical application of a surgical navigation system based on virtual laparoscopy in laparoscopic gastrectomy for gastric cancer. Int J Comput Assist Radiol Surg *11(5)*: 827-836, 2016. PMID: 26429785. DOI: 10.1007/s11548-015-1293-z

20 Pandey P, Guy P, Hodgson, AJ and Abugharbieh R: Fast and automatic bone segmentation and registration of 3D ultrasound to CT for the full pelvic anatomy: a comparative study. Int J Comput Assist Radiol Surg *13(10)*: 1515-1524, 2018. PMID: 29804181. DOI: 10.1007/s11548-018-1788-5

21 Ungi T, Abolmaesumi P, Jalal R, Welch M, Ayukawa I, Nagpal S, Lasso A, Jaeger M, Borschneck DP, Fichtinger G and Mousavi P: Spinal needle navigation by tracked ultrasound snapshots. IEEE Trans Biomed Eng *59(10)*: 2766-2772, 2012. PMID: 22851228. DOI: 10.1109/TBME.2012.2209881

Received October 30, 2020
Revised November 23, 2020
Accepted November 24, 2020